

Microstructure and high-temperature thermoelectric properties of polycrystalline $\text{CuAl}_{1-x}\text{Mg}_x\text{O}_2$ ceramics

K. Park^{a,*}, K.Y. Ko^a, J.K. Seong^a, S. Nahm^b

^a Department of Advanced Materials Engineering, Sejong University, Seoul 143-747, Republic of Korea

^b Department of Materials Science and Engineering, Korea University, Seoul 136-701, Republic of Korea

Available online 23 March 2007

Abstract

We investigated the effect of Mg-substitution on the microstructure and high-temperature thermoelectric properties of $\text{CuAl}_{1-x}\text{Mg}_x\text{O}_2$ ($0 \leq x \leq 0.2$) fabricated by the tape casting method. The sintered $\text{CuAl}_{1-x}\text{Mg}_x\text{O}_2$ bodies crystallized in $\text{CuAl}_{1-x}\text{Mg}_x\text{O}_2$ solid solutions along with MgAl_2O_4 and Cu_2MgO_3 phases. Mg substitution up to $x=0.12$ in the $\text{CuAl}_{1-x}\text{Mg}_x\text{O}_2$ yielded a higher electrical conductivity and lower Seebeck coefficient mainly because of an enhanced carrier density. The highest value of the power factor ($3.47 \times 10^{-5} \text{ W m}^{-1} \text{ K}^{-2}$) was attained for $\text{CuAl}_{0.88}\text{Mg}_{0.12}\text{O}_2$ at 800°C . It is demonstrated that Mg substitution is highly effective for improving high-temperature thermoelectric properties.

© 2007 Elsevier Ltd. All rights reserved.

Keywords: Pressing; Sintering; Electron microscopy; Electrical conductivity; MgO

1. Introduction

Thermoelectric materials with a high-energy conversion efficiency are strongly required for both electric power generation in terms of waste heat recovery and the refrigeration of electronic devices. The evaluation of the properties of thermoelectric materials can be expressed by figure-of-merit (Z) as follows¹: $Z = \sigma\alpha^2/\kappa$, where σ , α , and κ are the electrical conductivity, Seebeck coefficient, and thermal conductivity, respectively. Until now, it has been reported that thermoelectric materials such as PbTe, SiC, SiGe, and FeSi₂ show a high value of the high-temperature Z .^{1–5} However, they are easily decomposed or oxidized at high temperatures in air. Therefore, the practical utilization of these materials as power generators has been limited. Metal oxides have recently been studied as alternative thermoelectric materials because of their high thermal and chemical stability at high temperatures in air, easy manufacture, and low manufacturing cost.^{6–9} However, in general, the thermoelectric performance of the metal oxides is lower than that of the semiconductor alloys.

In 1997, Terasaki et al.⁶ reported a new thermoelectric material, NaCo_2O_4 , which has a high Z ($8.8 \times 10^{-4} \text{ K}^{-1}$) and a large α ($100 \mu\text{V K}^{-1}$) at 27°C . Since then, NaCo_2O_4 -based systems

have been extensively studied.^{6–9} However, their application is quite limited because of the volatility of sodium above 800°C and the hygroscopicity of NaCo_2O_4 in air.¹⁰ It is thus necessary to develop new oxide materials with both high performance and environmental stability. In this work, we have selected CuAlO_2 with a delafossite structure as a candidate material.^{11–13} Our approach to improve the thermoelectric performance is the partial substitution of Mg for Al in CuAlO_2 . In the present study, the thermoelectric properties of the $\text{CuAl}_{1-x}\text{Mg}_x\text{O}_2$ ($0 \leq x \leq 0.2$) ceramics fabricated by the tape casting method were studied, especially with regard to the substitution of Mg for Al. Tape casting is the prominent process used to produce thin and flat ceramic sheets mainly for the electronic industry.¹⁴

2. Experimental

All samples of $\text{CuAl}_{1-x}\text{Mg}_x\text{O}_2$ ($x=0, 0.04, 0.08, 0.12, 0.16$, and 0.2) were fabricated by the tape casting method starting from high-purity CuO, Al_2O_3 , and MgO powders. A mixture of the CuO, Al_2O_3 , and MgO powders and ethyl alcohol was milled for 6 h using a planetary mill (FRITSCH pulverisette 6) and ZrO_2 ball as a grinding media. The obtained slurries were dried at 80°C in an oven for 12 h. Subsequently, the mixed powders were calcined in a mullite crucible at 1000°C for 5 h. The calcined powders were milled in the planetary mill for 6 h and dried at 80°C in an oven for 12 h. After the powders were mixed

* Corresponding author. Tel.: +82 2 3408 3777; fax: +82 2 3408 3664.
E-mail address: kspark@sejong.ac.kr (K. Park).

with solvents (toluene and ethyl alcohol) and a dispersant (BYK, BYK Chemie GmbH, Wesel, Germany) in a ball mill for 12 h, plasticizers (polyethylene glycol 400, polyethylene glycol 3350, di-octyl phthalate, and ethylene glycol) and a binder (polyvinyl butyral) were added into the mixture and then mixed for another 24 h. The obtained slurry was degassed in vacuum to remove gas bubbles and then tape cast onto a plastic film with a laboratory tape caster (STC-14A, Hansung Systems, Korea) at a temperature of 75 °C and at a speed of 600 mm/min with a blade opening of 250 μm. The pieces were then stacked and laminated by pressing at 50 MPa and 75 °C for 10 min. The resulting compacts were heated at 1200 °C for 20 h in air and then furnace cooled.

The crystal structure of the as-sintered $\text{CuAl}_{1-x}\text{Mg}_x\text{O}_2$ ($0 \leq x \leq 0.2$) samples was analyzed with an X-ray diffractometer (XRD; Rigaku DMAX-2500) using Cu K α radiation at 40 kV and 100 mA. The microstructure of the as-sintered samples was investigated by a scanning electron microscope (SEM; Hitachi S4700). In order to measure the thermoelectric properties as a function of temperature, the electrical conductivity σ and the Seebeck coefficient α were simultaneously measured over a temperature range of 450–800 °C. The samples for the measurements of thermoelectric properties were cut out of the sintered bodies in the form of rectangular bars of 2 mm × 2 mm × 15 mm with a diamond saw and polished with SiC emery papers. After four grooves were put on the rectangular bars, Pt wires were wound along the grooves. Further details on thermoelectric property measurements may be found elsewhere.¹¹

3. Results and discussion

Fig. 1(a)–(c) show the XRD patterns of the as-sintered CuAlO_2 , $\text{CuAl}_{0.88}\text{Mg}_{0.12}\text{O}_2$, and $\text{CuAl}_{0.8}\text{Mg}_{0.2}\text{O}_2$ samples, respectively. The crystal structure of the sintered CuAlO_2 bodies is rhombohedral, $R\bar{3}m$, with a lattice constant of $a = 2.8567 \text{ \AA}$ and $c = 16.943 \text{ \AA}$,¹² in conformity with that previously reported for this material.^{11,13} For the Mg substituted $\text{CuAl}_{1-x}\text{Mg}_x\text{O}_2$, in addition to the CuAlO_2 , second phases MgAl_2O_4 and Cu_2MgO_3

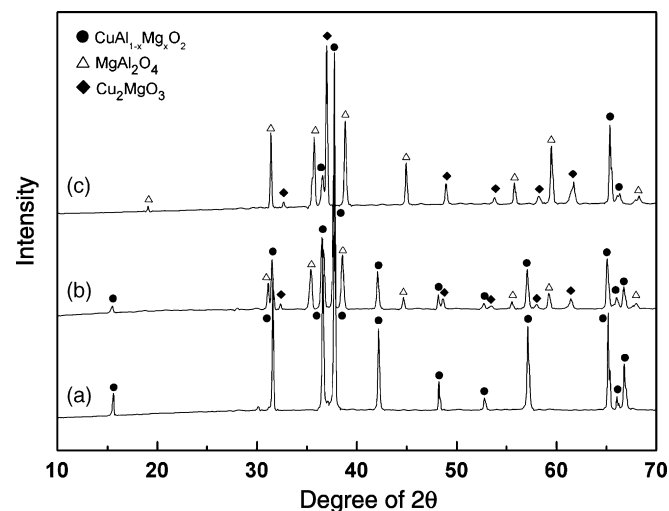


Fig. 1. XRD patterns of the as-sintered (a) CuAlO_2 , (b) $\text{CuAl}_{0.88}\text{Mg}_{0.12}\text{O}_2$, and (c) $\text{CuAl}_{0.8}\text{Mg}_{0.2}\text{O}_2$ samples.

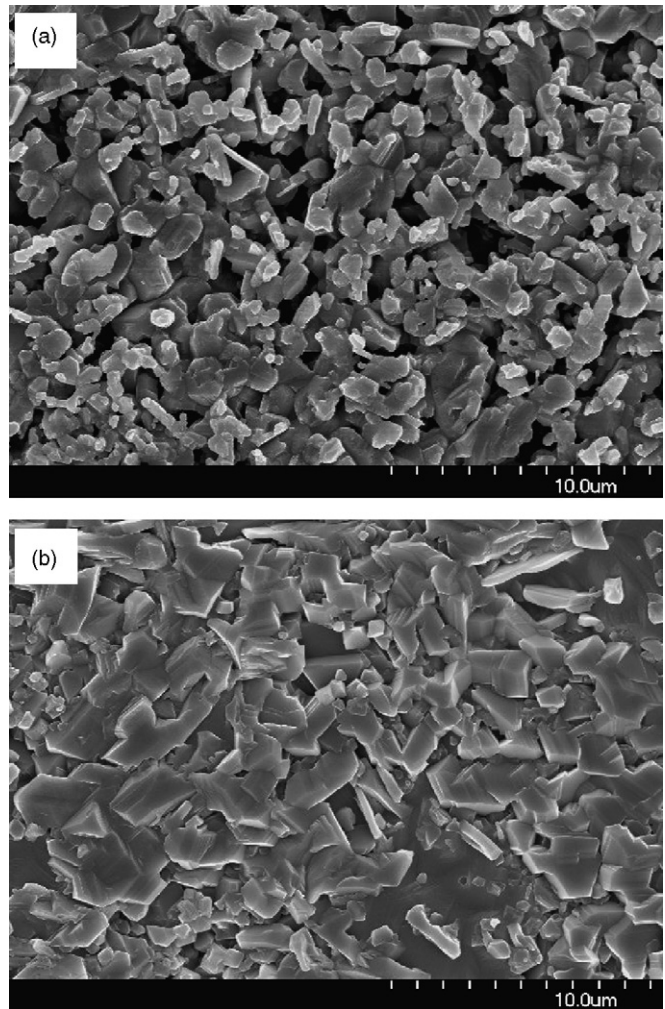


Fig. 2. SEM images from the surface of the as-sintered (a) CuAlO_2 and (b) $\text{CuAl}_{0.88}\text{Mg}_{0.12}\text{O}_2$ samples.

were detected. MgAl_2O_4 belongs to the space group $Fd\bar{3}m$ (227) and has the spinel cubic structure ($a = 8.083 \text{ \AA}$).¹⁵ Also, the crystal structure of Cu_2MgO_3 is monoclinic with a lattice constant of $a = 40.534 \text{ \AA}$, $b = 3.995 \text{ \AA}$, and $c = 3.183 \text{ \AA}$.¹⁶ The intensity of second phases MgAl_2O_4 and Cu_2MgO_3 becomes stronger with an increase in Mg content.

Fig. 2(a) and (b) show the SEM images from the surface of the as-sintered CuAlO_2 and $\text{CuAl}_{0.88}\text{Mg}_{0.12}\text{O}_2$ samples, respectively. The grain size and density were found to be gradually greater by increasing the MgO content. This could be due to the fact that the substituted Mg acts as a sintering additive and the Mg substitution leads to a rise in the activity of CuAlO_2 as a consequence of the distortion of the CuAlO_2 lattice, which is beneficial to grain growth in Mg-substituted $\text{CuAl}_{1-x}\text{Mg}_x\text{O}_2$ samples.¹⁷ In addition, most pores exist at the grain boundaries, and some also remain within individual grains.

The temperature dependence of the electrical conductivity σ for the $\text{CuAl}_{1-x}\text{Mg}_x\text{O}_2$ ($0 \leq x \leq 0.2$) samples is shown in Fig. 3. The electrical conductivity increased with temperature over the measured temperature range, indicating a semiconducting behavior. It is apparent that the incorporation of MgO to CuAlO_2 up to $x = 0.12$ yields higher electrical conductivity. This

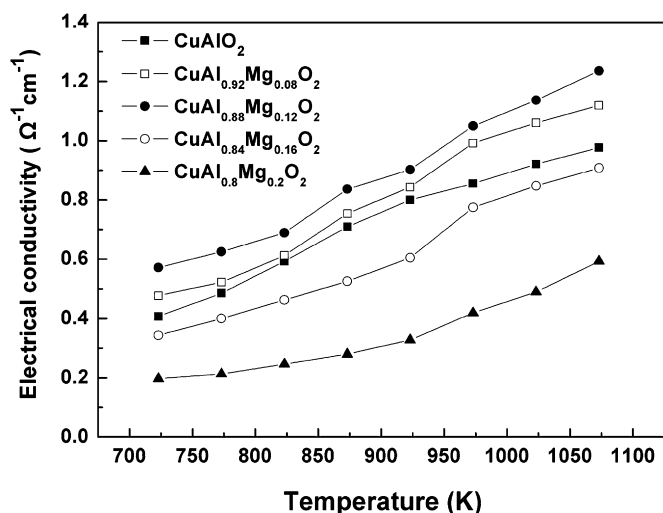


Fig. 3. Temperature dependence of the electrical conductivity for the $\text{CuAl}_{1-x}\text{Mg}_x\text{O}_2$ ($0 \leq x \leq 0.2$) samples.

can be explained by considering the following various competing factors on the electrical conductivity. (1) The substitution of Mg^{2+} for Al^{3+} may increase the hole concentration of the system to compensate for the electric charge balance, resulting in an increase in the electrical conductivity. (2) The amount of MgAl_2O_4 and Cu_2MgO_3 phases with a low electrical conductivity becomes more prominent with Mg content, thereby lowering the electrical conductivity. (3) The porosity and grain boundary areas, which are responsible for the decrease in the time between scattering events of charge carriers, decreased with increasing Mg content, thereby enhancing the electrical conductivity. From the above competing factors, it can be considered that the increased electrical conductivity as a consequence of MgO addition up to $x=0.12$ is mainly due to an enhanced hole concentration, density, and grain size of the system. We believe that MgO addition is fairly effective in achieving high conductivity. In addition, the electrical conductivity of $\text{CuAl}_{1-x}\text{Mg}_x\text{O}$ samples with a high Mg content ($x \geq 0.16$) was lowered with an increase in Mg content. This mainly originates from an increase in the amount of MgAl_2O_4 and Cu_2MgO_3 phases with a high electrical resistivity.

Fig. 4 shows the Seebeck coefficient α of the $\text{CuAl}_{1-x}\text{Mg}_x\text{O}_2$ ($0 \leq x \leq 0.2$) samples as a function of temperature. The sign of the Seebeck coefficient is positive for all the measured temperature ranges, indicating that the major conductivity carriers are holes. The values of the Seebeck coefficient for the $\text{CuAl}_{1-x}\text{Mg}_x\text{O}_2$ samples are lowered with increasing temperature and then become greater. In addition, Mg substitution up to $x=0.12$ lowers the Seebeck coefficient with Mg content, suggesting that the carrier density increased by means of the Mg substitution. In general, the value of the Seebeck coefficient becomes smaller with increasing carrier density in common semiconductors.¹ The Seebeck coefficient of the $\text{CuAl}_{1-x}\text{Mg}_x\text{O}$ samples with high Mg content ($x \geq 0.16$) was enhanced at the higher Mg content mainly because the amount of MgAl_2O_4 and Cu_2MgO_3 phases having a high Seebeck coefficient became more pronounced.

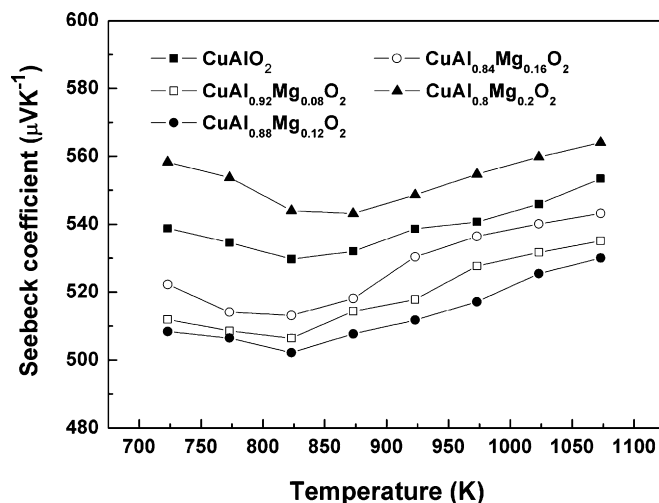


Fig. 4. Seebeck coefficient of the $\text{CuAl}_{1-x}\text{Mg}_x\text{O}_2$ ($0 \leq x \leq 0.2$) samples as a function of temperature.

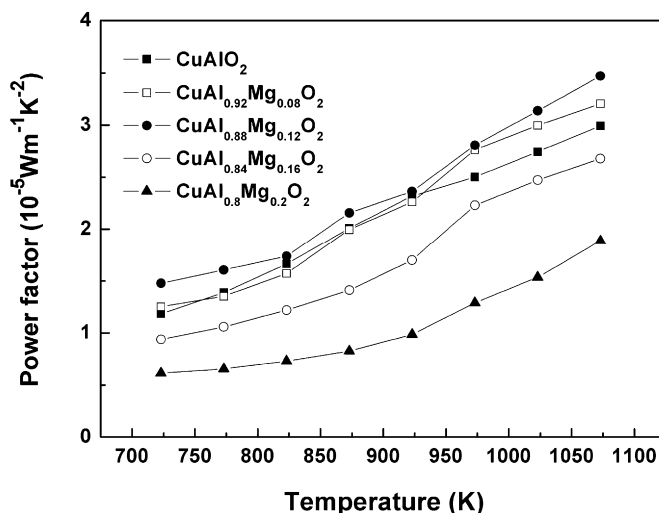


Fig. 5. Power factor of the $\text{CuAl}_{1-x}\text{Mg}_x\text{O}_2$ ($0 \leq x \leq 0.2$) samples as a function of temperature.

The power factor $\sigma\alpha^2$ calculated from the data in Figs. 3 and 4 is plotted in Fig. 5. The power factor of the $\text{CuAl}_{1-x}\text{Mg}_x\text{O}_2$ ($0 \leq x \leq 0.2$) samples becomes greater with an increase in temperature. Mg substitution up to $x=0.12$ at high temperatures ($\geq 700^\circ\text{C}$) yields a higher power factor because it significantly enhances the electrical conductivity. The highest value of the power factor ($3.47 \times 10^{-5} \text{ W m}^{-1} \text{ K}^{-2}$) was attained for $\text{CuAl}_{0.88}\text{Mg}_{0.12}\text{O}_2$ at 800°C . In addition to high power factors, the Mg-substituted $\text{CuAl}_{1-x}\text{Mg}_x\text{O}_2$ ceramics have advantages for use in thermoelectric devices, i.e., thermal and chemical stability under air or oxidizing atmospheres at high temperatures.

4. Conclusions

Polycrystalline $\text{CuAl}_{1-x}\text{Mg}_x\text{O}_2$ ($0 \leq x \leq 0.2$) samples were fabricated by the tape casting method. The sintered $\text{CuAl}_{1-x}\text{Mg}_x\text{O}_2$ bodies contained a $\text{CuAl}_{1-x}\text{Mg}_x\text{O}_2$ solid solution with a rhombohedral structure, $R\bar{3}m$, along with MgAl_2O_4

and Cu_2MgO_3 phases. The density and grain size became greater with MgO content. Mg substitution up to $x=0.12$ in the $\text{CuAl}_{1-x}\text{Mg}_x\text{O}_2$ yielded a higher electrical conductivity and lower Seebeck coefficient mainly because of an enhanced hole concentration of the system. The power factor up to $x=0.12$ at high temperatures ($\geq 700^\circ\text{C}$) was substantially increased by means of Mg substitution because the electrical conductivity became greater. The highest value of the power factor ($3.41 \times 10^{-5} \text{ W m}^{-1} \text{ K}^{-2}$) was attained for $\text{CuAl}_{0.88}\text{Mg}_{0.12}\text{O}_2$ at 800°C . In conclusion, the partial substitution of Mg for Al in CuAlO_2 was highly effective for improving high-temperature thermoelectric properties.

Acknowledgement

The authors would like to acknowledge the financial support provided for this research by the Korea Energy Management Corporation (KEMCO).

References

1. Bhandari, C. M. and Rowe, D. M., Optimization of carrier concentration. In *CRC handbook of thermoelectrics*, ed. D. M. Rowe. CRC Press, Boca Raton, 1995.
2. Ito, M., Seo, W.-S. and Koumoto, K., Thermoelectric properties of PbTe thin films prepared by gas evaporation method. *J. Mater. Res.*, 1999, **14**, 209–212.
3. Pai, C. H., Sasaki, Y. and Koumoto, K., Reaction sintering of polycarbosilane-impregnated compact of silicon carbide hollow particles and the resultant thermoelectric properties. *J. Am. Ceram. Soc.*, 1991, **74**, 2922–2924.
4. Vining, C. B., Laskow, W., Hanson, J. O., Van der Beck, R. R. and Gorsuck, P. D., Thermoelectric properties of pressure-sintered $\text{Si}_{0.8}\text{Ge}_{0.2}$ thermoelectric alloys. *J. Appl. Phys.*, 1991, **69**, 4333–4340.
5. Cho, W.-S., Choi, S.-W. and Park, K., Microstructure and thermoelectric properties of *p*-type $\text{Fe}_{0.9}\text{Mn}_{0.1}\text{Si}_2$ compounds prepared by pressureless sintering. *Mater. Sci. Eng. B*, 1999, **68**, 116–122.
6. Terasaki, I., Sasago, Y. and Uchinokura, K., Large thermoelectric power in NaCo_2O_4 single crystals. *Phys. Rev. B*, 1997, **56**, R12685–R12687.
7. Terasaki, I., Transport properties and electronic states of the thermoelectric oxide NaCo_2O_4 . *Phys. B*, 2003, **328**, 63–67.
8. Fujita, K., Mochida, T. and Nakamura, K., High-temperature thermoelectric properties of $\text{Na}_x\text{CoO}_{2-8}$ single crystals. *Jpn. J. Appl. Phys.*, 2001, **40**, 4644–4647.
9. Ando, Y., Miyamoto, N., Segawa, K., Kawata, T. and Terasaki, I., Specific-heat evidence for strong electron correlations in the thermoelectric material $(\text{Na,Ca})\text{Co}_2\text{O}_4$. *Phys. Rev. B*, 1999, **60**, 10580–10583.
10. Terasaki, I., Physical properties of NaCo_2O_4 and the related oxides: strongly correlated layered oxides as thermoelectric materials. In *Proceedings of the 18th International Conference on Thermoelectrics*, International Thermoelectric Society, 1999, pp. 569–576.
11. Park, K., Ko, K. Y. and Seo, W.-S., Thermoelectric properties of CuAlO_2 . *J. Eur. Ceram. Soc.*, 2005, **25**, 2219–2222.
12. JCPDS Card File: 35-1401.
13. Shannon, R. D., Rogers, D. B. and Prewitt, C. T., Chemistry of noble metal oxides. I. Syntheses and properties of ABO_2 delafossite compounds. *Inorg. Chem.*, 1971, **10**, 713–718.
14. Pagnoux, G., Chartier, T., Granja, M. de F., Doreau, F. and Ferreira, J. M., Aqueous suspensions for tape-casting based on acrylic binders. *J. Eur. Ceram. Soc.*, 1998, **18**, 241–247.
15. JCPDS Card File: 21-1152.
16. JCPDS Card File: 41-1381.
17. Zhu, B. L., Xie, C. S., Wang, W. Y., Huang, K. J. and Hu, J. H., Improvement in gas sensitivity of ZnO thick film to volatile organic compounds (VOCs) by adding TiO_2 . *Mater. Lett.*, 2004, **58**, 624–629.